EGU2011-3614 (XL214)

Cryogenic EBSD: a technique to preserve a stable surface in a low pressure SEM to characterize ice microstructure

I. Weikusat (ilka.weikusat@awi.de), D.A.M. De Winter, G. M. Pennock, M. Hayles, C.T.W.M. Schneijdenberg, M. R. Drury
AWI, Bremerhaven, Germany; Utrecht University, Utrecht, The Netherlands; FEI Co. Nanoport, Eindhoven, The Netherlands

Introduction

The characterization and localization of subgrain boundaries (sGB) in typically coarse-grained polar ice requires good correlation of light microscopy (LM) and EBSD mapping, which needs a stable sample surface avoiding alteration by (e.g.) sublimation during the measurement.

Sample Transfer

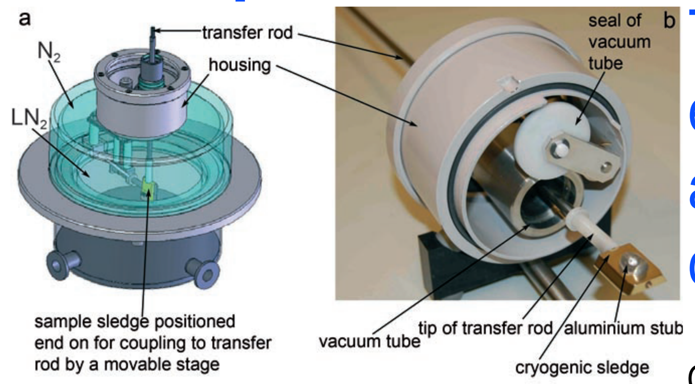

The sample is never exposed to warm atmosphere air during transfer.

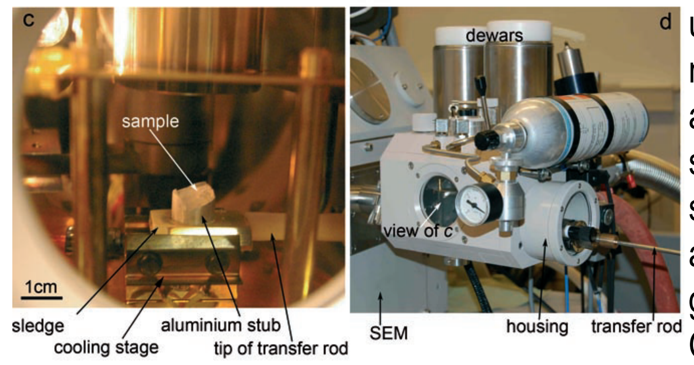

Cryo-transfer system. (a) Transfer unit (LN$_2$ = liquid nitrogen, N$_2$ = nitrogen gas). (b) Transfer rod and sample holder. (c) View into specimen preparation chamber; sample mounted on a pretilted aluminium stub fitting in the cryo-genic sledge. (d) Complete Quorum preparation chamber.

SEM & EBSD Conditions

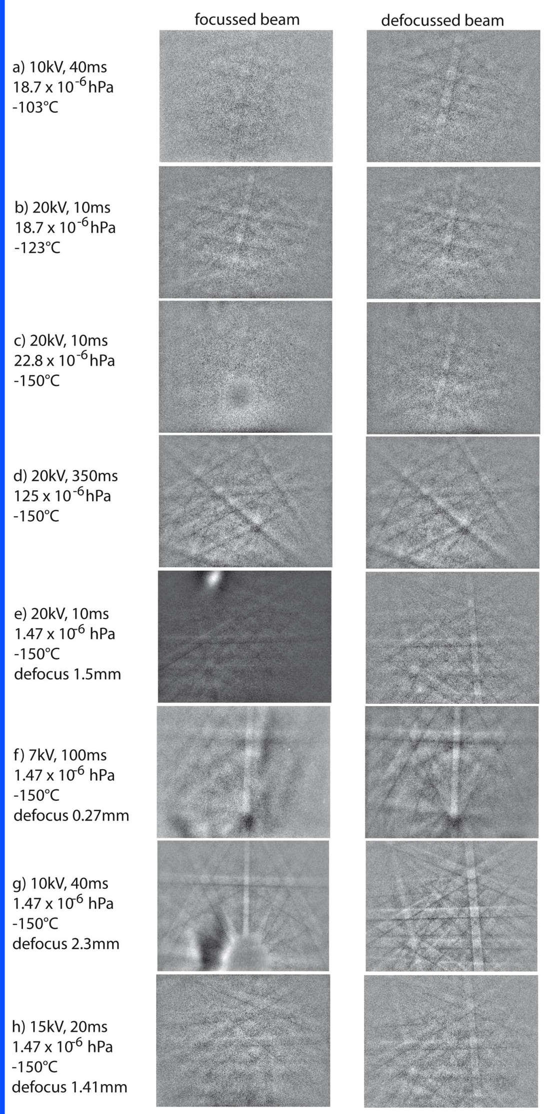

EBSPs with focused and defocused beam. (a)–(d) High P conditions using N$_2$ gas. (e)–(h) Low P conditions. Acc. voltage, time/frame for pattern collection, chamber P and T given. Mapping step size 5 µm, grid size 10×10. Values for defocus, where noted, given.

SEM chamber pressure (P) and temperature (T) conditions chosen within the ice stability P-T-field enable the preservation of a stable surface for good correlation with LM. Instead of sublimation, beam defocus is used as charge minimizer. EBSP quality and grid distortion can be improved significantly. Defocusing changes the spatial resolution slightly, which is however still far below the scales of the envisaged substructres.

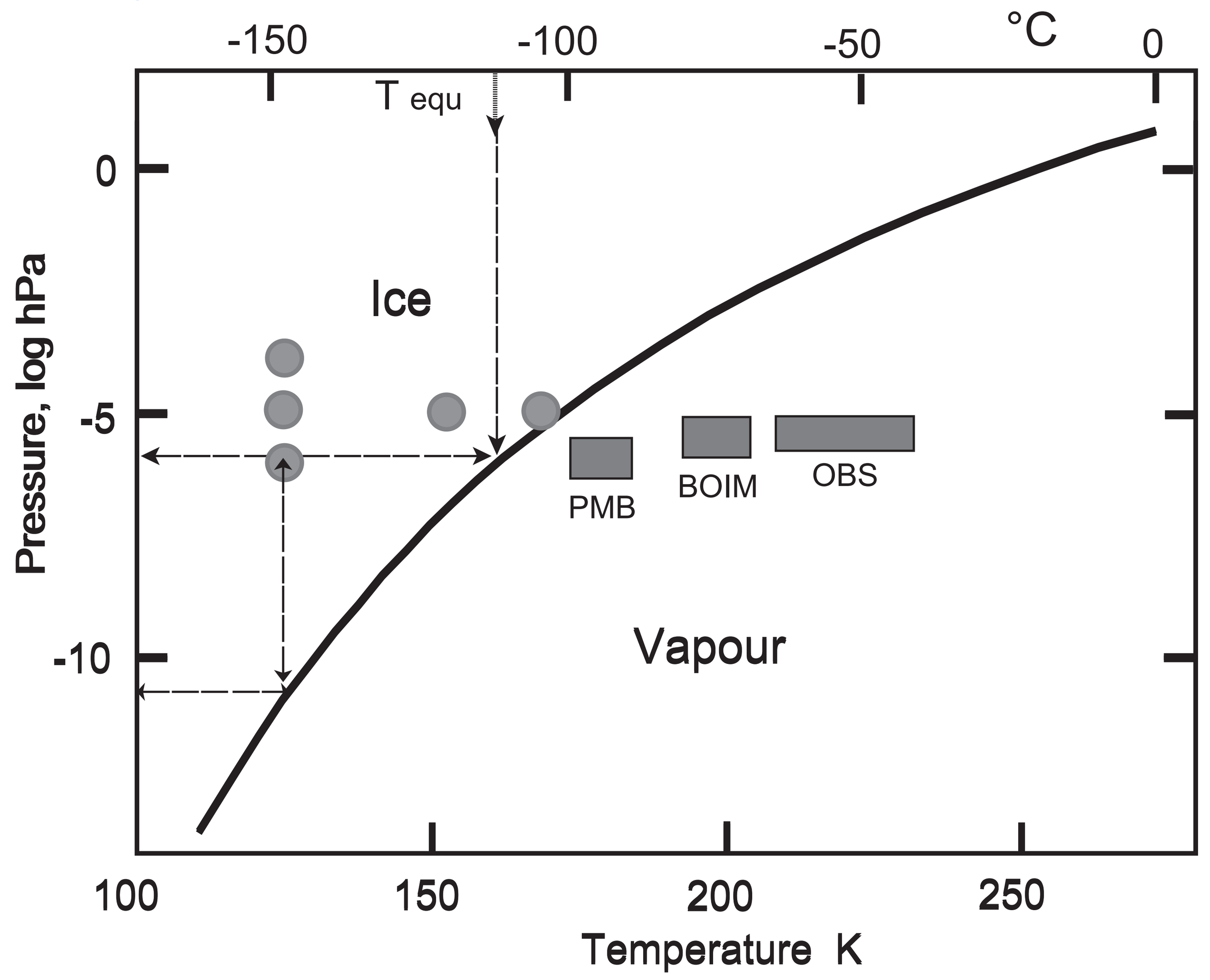

Equilibrium phase diagram (P-T) of stability conditions for ice and ice in equilibrium with water vapour in a closed system (after Andreas,2007). SEM chamber P and stage T conditions of published EBSD studies on ice shown as blocks: (PMB=Piazolo EA, 2008; BOIM=Baker EA,2007; OBS=Obbard EA, 2006). Typical SEM chamber P and T conditions examined here (Weikusat EA,2010) shown as circles. Equilibrium T_{equ} for chamber P of 10^{-6} hPa is ca. -112°C (shown). Partial vapour P_{equ} (shown) for a lower stage temperature of -150°C is much lower than the chamber P.

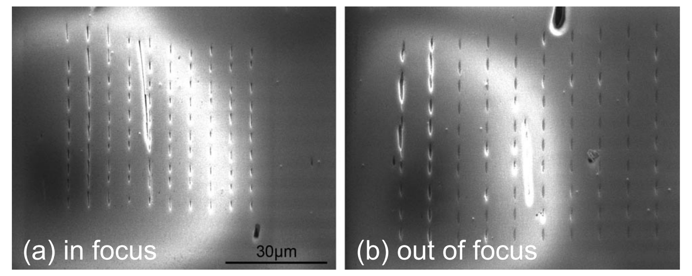

Grid of damage spots, caused by e-beam. EBSD map settings identical: 10 kV acc. voltage, 40ms/frame for pattern collection, 1.4×10^{-5} hPa chamber P, -103°C chamber T. Distortion of grid is significantly less in (b). Note, 5 µm step size as set, is actually slightly changed giving a slightly larger spot distance in (b). Accurate resolution and scale for maps has to be determined from an SE image taken after the mapping.

EBSD & LM Correlation

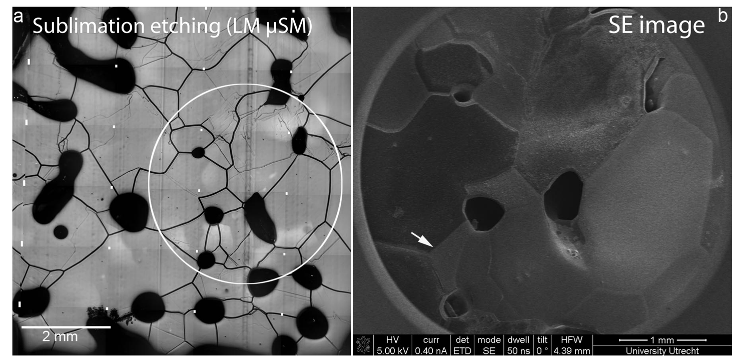

Locating region of interest in the SEM (sample B37, 93.9 m depth). (a) showing boundary and pore features (Kipfstuhl EA,2006). (b) corresponding area indicated as circle in (a). Most grains have the same shape: one boundary (arrowed) has slightly altered position.

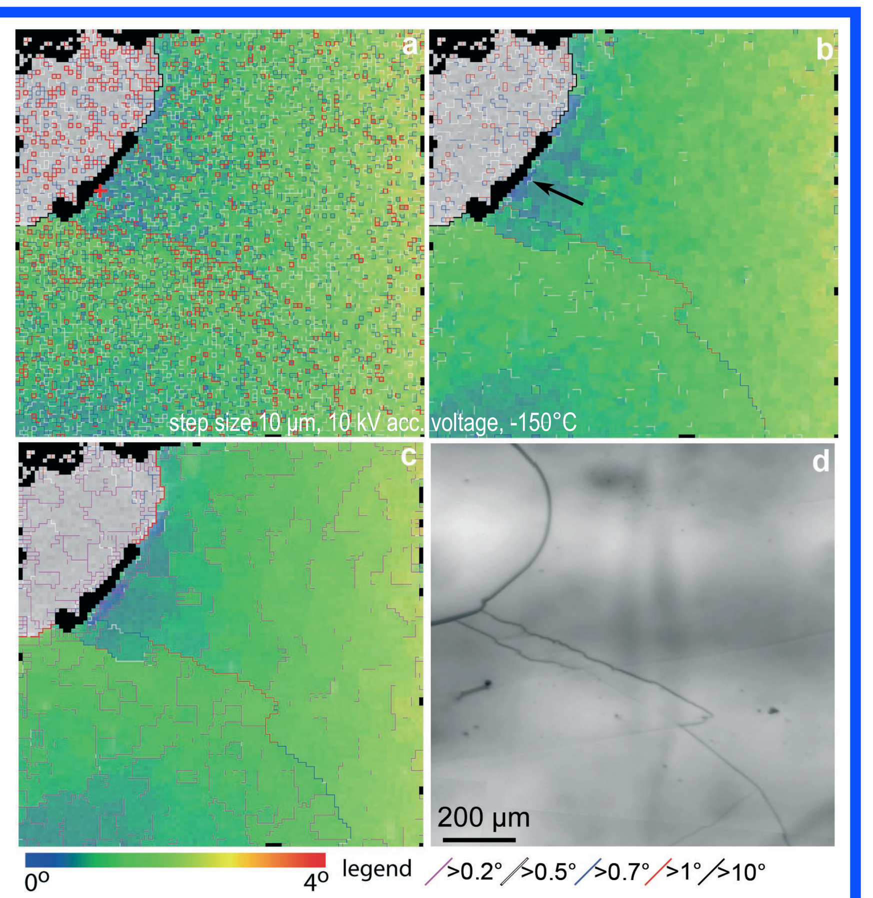

EBSD and LM mapped microstructure (sample EDML 2575.8m depth). (a) Map after replacement of some nonindexed pixels and all misindexed pixels . Etched GB is poorly indexed. Lower grain shows a slight orientation gradient. (b) After orientation averaging (2 passes of 3×3 filter) most low angle noise is removed to show sGB penetrating several 100s of µm into the core of the grain. Filtering removes low angle misorientation noise but also creates a low angle boundary artefact (arrow). (c) After orientation averaging (2 passes of 5×5 filter) boundaries of 0.2-0.5° are also artefacts of the orientations averaging filter. Angular resolution is ca. 0.7° after orientation averaging. (d) Corresponding etched LM µS.

Localization of relevant features, demanding esp. in very coarse-grained deep ice, is enabled by pre-scanning with LM microstructure mapping. Comparison with these etch features allows orientation averaging as noise reduction method. Correlation of LM with EBSD microstructure is excellent.

Sample Surface

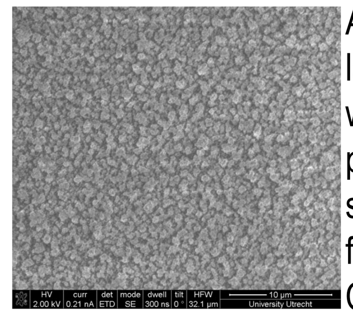

After transfer: irregular layer of frost crystals with cauliflower morphology (Zone 1 of structure zone model for growth of ice films; Cartwright EA,2010).

Cauliflower frost after transfer is removed by controlled sublimation in the prep. chamber leading to surface faceting. Sublimation is carried out before exposition to e-beam, which changes sublimation/condensation behavior.

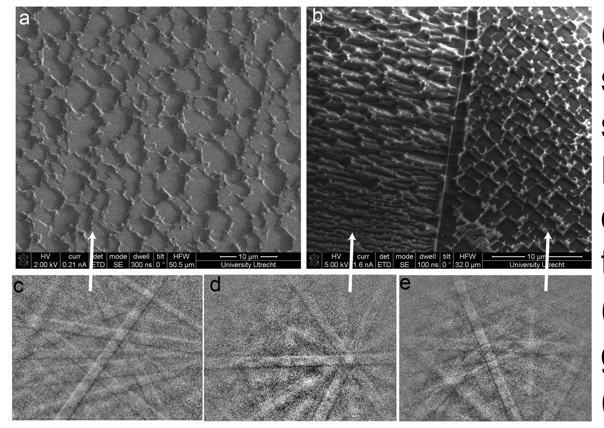

(a) & (b) Faceted surfaces after sublimation. Faceting depends on crystal orientation). (c)-(e) EBSPs from grains in (a) resp. (b).

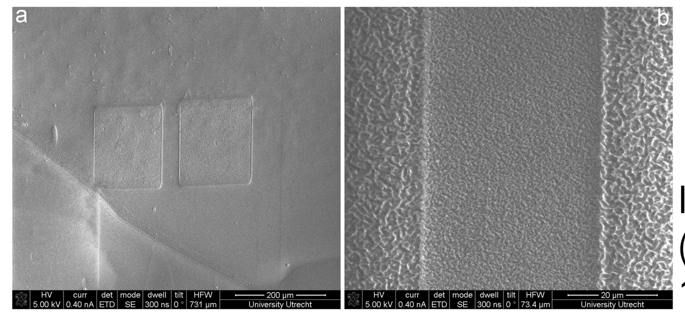

Influence of beam exposure to surface topography. Sample was sublimed after area scanning. (a) Areas exposed to e-beam clearly stand out as squares (left: 20 min @ 10 kV, right: 30 min @ 10 kV). (b) Detail of (a) showing preexposed areas and the only sublimed surface (band in middle).

References:
Weikusat et al. 2011, Subgrain boundaries in Antarctic ice quantified by X-ray Laue diffraction, J. Glaciol., 57, 85-94.
Cartwright et al., 2010, Ice films follow structure zone model morphologies, Thin Solid Films, 518, 3422-3427.
Weikusat et al. 2010, Cryogenic EBSD on ice: preserving a stable surface in a low pressure SEM, J. Microsc., doi: 10.1111/j.1365-2818.2010.03471.x.
Piazolo et al. 2008, Sub-structure characterization of experimentally and naturally deformed ice using cryo-EBSD, J. Microsc., 230, 509-51.
Baker et al., 2007, Microstructural characterization of firn. Hydrol. Process., 21, 1624-1629.
Andreas, 2007, New estimates for the sublimation rate for ice on the Moon. Icarus, 186, 24-30.
Obbard et al. 2006, Using electron backscatter diffraction patterns to examine recrystallization in polar ice sheets. J. Glaciol., 52, 546-557.
Kipfstuhl et al. 2006, Microstructure mapping: a new method for imaging deformation induced microstructural features of ice on the grain scale. J. Glaciol., 52, 398-406.

Spatial Resolution

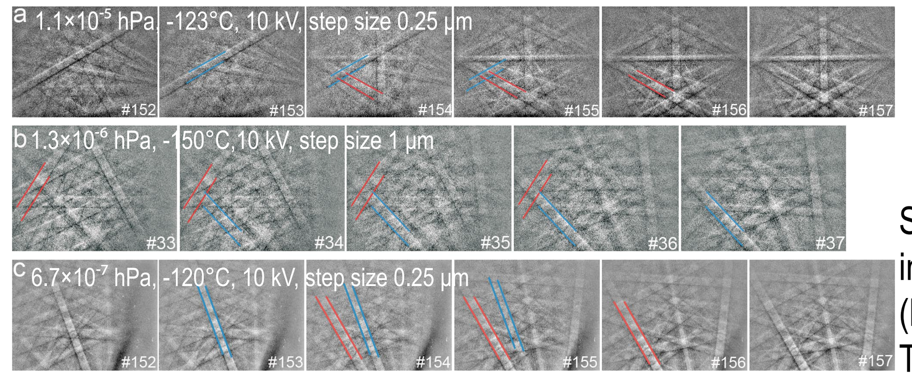

Spatial resolutions depend on exact P-T conditions. They are between 0.5 and 3 µm. Substructure spacing is typically above 10 µm.

Sequential EBSPs across vertical GB. Slightly defocused beam. (a) High P.Two images (#154 – 155) show bands from both patterns of neighbouring grains. (b) Low P. Three images (#34–36) show bands from both patterns . (c) Low P. Three images (#154 – 155) show bands from both patterns.

Reproducibility

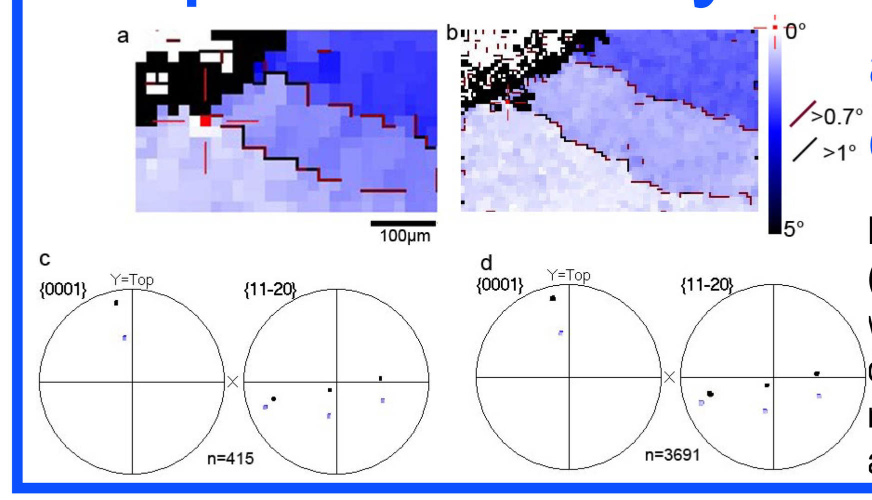

Excellent reproducibility of structures, orientations and indexing can be achieved if sublimation/condensation is minimized (see also Sample Surface).

EBSD mappping reproducibility (sample EDML 2575.8 m depth). (a) EBSD map (step size 10 µm) (b) second EBSD map of same area (step size 1 µm). Indexing was 87% and 88% resp. (without offline reanalysis). (c) Stereographic projection of data in (a). (d) Stereographic projection of data in (b). Acc. voltage 10 kV. Noise reduction of both maps was made by replacement of some nonindexed pixels and all misindexed pixels and one pass of a 3×3 modified Kuwahara filter.

Example for Substructure Characterization

EBSD analysis (sample EDML 655.9 m depth). (a) Map with subsets along sGB highlighted. sGB types are labelled 1–3. (b) Stereographic projections of c- and a-axes. (c) Rotation axes among neighbouring pixels with misorientation >0.5° in sGB subsets. Labels 1–3 correspond to labels in (a). (d) Simplified interpretation (following Weikusat EA,2011).

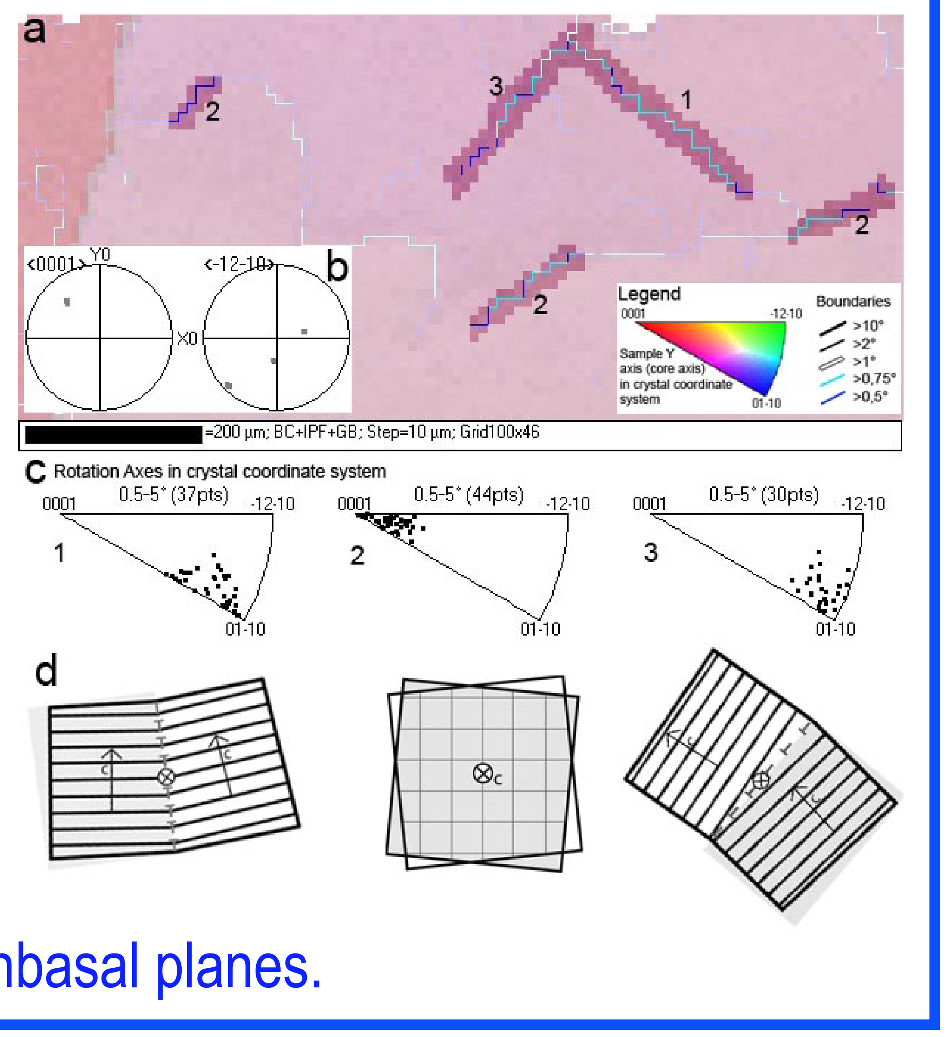

sGB can be characterized:
(1) tilt boundaries comprised of edge dislocations gliding in basal plane, (2) twist boundaries built by basal screw dislocation sets and (3) tilt boundaries comprised of edge dislocations gliding on nonbasal planes.